Published in final edited form as:
Metabolism. 2013 December ; 62(12): 1850–1857. doi:10.1016/j.metabol.2013.08.003.

Early Detection of Liver Steatosis by Magnetic Resonance Imaging in Rats Infused with Glucose and Intralipid Solutions and Correlation to Insulin Levels

Gaspard d'Assignies[1,2,3], **Ghislaine Fontés**[2,4,5], **Claude Kauffmann**[1,2], **Martin Latour**[2,4], **Louis Gaboury**[8], **Yvan Boulanger**[1,2], **Bernard E. Van Beers**[3], **Gilles Soulez**[9], **Vincent Poitout**[2,4,5,6,7], and **An Tang**[1,2]

[1]Department of Radiology, University of Montreal, Hôpital Saint-Luc, 1058 rue Saint-Denis, Montreal, Quebec, Canada, H2X 3J4

[2]Research Center CHUM, Hôpital Saint-Luc, 264, René-Lévesque Blvd. East, Montreal, Quebec, Canada, H2X 1P1

[3]Department of Radiology, Beaujon Hospital, Université Paris VII, 100 Bd du Général Leclerc, 92118 Clichy, France

[4]Montreal Diabetes Research Center, CRCHUM, Technopôle Angus, 2901, Rachel Street East – Room 303, Montreal, Quebec, Canada, H1W 4A4

[5]Department of Medicine, University of Montreal, Qc, Canada, PO Box 6128, Station Centre-ville, Montreal, Quebec, Canada, H3C 3J7

[6]Department of Nutrition, University of Montreal, Qc, Canada, PO Box 6128, Station Centre-ville, Montreal, Quebec, Canada, H3C 3J7

[7]Department of Biochemistry, University of Montreal, Qc, Canada, PO Box 6128, Station Centre-ville, Montreal, Quebec, Canada, H3C 3J7

[8]Department of anatomo-pathology, Centre hospitalier de l'Université de Montréal (CHUM), 3840 rue St-Urbain, Montreal, Quebec, Canada, H2W 1T8

[9]Department of Radiology, University of Montreal, Hôpital Notre-Dame, 1560 rue Sherbrooke Est, Montreal, Quebec, Canada, H2L 4M1

Abstract

Objective—Magnetic resonance (MR) techniques allow noninvasive fat quantification. We aimed to investigate the accuracy of MR imaging (MRI), MR spectroscopy (MRS) and

Corresponding author: An Tang, MD, MSc, FRCPC, Department of Radiology, University of Montreal and CRCHUM, Hôpital Saint-Luc, 1058 rue Saint-Denis, Montréal, Québec, Canada, H2X 3J4, Telephone: (514) 944-444-4213, Fax: (514) 412-7359, Duotango@gmail.com.

Disclosure statement: We have no conflict of interest to report.

Author contributions: G.d'A., G.F., M.L., V.P., and A.T. participated in the design of the study; G.d'A. and G.F., performed the statistical analysis; G.d'A., G.F., C.K., M.L., L.G., Y.B., and A.T. participated in acquisition of the data; G.d'A, Y.B., B.V.B., G.S., V.P., and A.T. participated in the interpretation of the data and drafted the manuscript. All authors read and approved the final manuscript.

histological techniques to detect early-onset liver steatosis in three rat phenotypes assigned to an experimental glucolipotoxic model or a control group.

Materials and Methods—This study was approved by the institutional committee for the protection of animals. Thirty-two rats (13 young Wistar, 6 old Wistar and 13 diabetic Goto-Kakizaki rats) fed a standard diet were assigned to a 72 h intravenous infusion of glucose and Intralipid fat emulsion or a saline infusion. Plasma insulin levels were measured. Steatosis was quantified in *ex vivo* livers with gradient-recalled multi-echo MRI, MRS and histology as fat fractions (FF).

Results—A significant correlation was found between multi-echo MRI-FF and MRS-FF ($r = 0.81$, $p < 0.01$) and a weaker correlation was found between histology and MRS-FF ($r = 0.60$, $p < 0.01$). MRS and MRI accurately distinguished young Wistar and Goto-Kakizaki rats receiving the glucose + Intralipid infusion from those receiving the saline control whereas histology did not. Significant correlations were found between MRI or MRS and insulin plasma level ($r = 0.63$, $p < 0.01$; $r = 0.57$, $p < 0.01$), and between MRI or MRS and C-peptide concentration ($r = 0.54$, $p < 0.01$; $r = 0.44$, $p < 0.02$).

Conclusions—Multi-echo MRI and MRS may be more sensitive to measure early-onset liver steatosis than histology in an experimental glucolipotoxic rat model.

Keywords

Hepatic steatosis; nonalcoholic fatty liver disease; MRI; diabetes mellitus; insulin

1. Introduction

Type 2 diabetes mellitus is closely linked to nonalcoholic fatty liver disease (NAFLD), characterized by increased lipid accumulation in the liver. Recent longitudinal studies suggest that NAFLD precedes and increases the risk of developing type 2 diabetes [1, 2]. Conversely, patients with type 2 diabetes have 80% more liver fat than age- and weight-matched nondiabetic subjects [3].

NAFLD associated with metabolic syndrome is an independent predictor of all-cause, liver specific and cardiovascular mortality [4]. On liver pathology, association between NAFLD and type 2 diabetes is related to a worse prognosis of hepatic necroinflammation and fibrosis [5-8]. If left untreated, 20% of fatty liver patients will progress to nonalcoholic steatohepatitis (NASH) and about 10% of NASH patients will progress to cirrhosis [9]. Moreover, the incidence of hepatocellular carcinoma doubles in patients with type 2 diabetes compared to controls, contributing to the dramatic rise in the incidence of hepatocellular carcinoma observed in recent years [10]. In this epidemiological context, early detection and better understanding of the relationship between type 2 diabetes/glucose metabolism and fatty liver is crucial [11, 12].

Histological analysis of a liver biopsy sample remains the current reference standard for liver fat quantification despite several well-known limitations [13-15], especially the invasive nature of the procedure which prevents dynamic monitoring of the disease at multiple time points.

Magnetic resonance (MR) techniques are accurate noninvasive modalities for quantification of hepatic steatosis, as reported in many recent studies [16, 17]. Among the MR-based fat quantification methods proposed [18, 19], proton magnetic resonance spectroscopy (MRS) has emerged as the noninvasive reference standard, often replacing histology. However, the technique is complex, requires spectroscopy expertise, and is not available on all MR scanners. Multi-echo MR imaging (MRI) methods are more widely available and allow for

fat quantification with T2* correction to improve accuracy. The accuracy of MRI techniques is known to be close to that of MRS in patients with NAFLD or type 2 diabetes [20, 21]. To assess early steatosis in an experimental glucolipotoxic model, we used a preclinical rodent model of nutrient-induced insulin resistance and pancreatic beta-cell dysfunction (glucolipotoxicity) with or without pre-existing diabetes, consisting of 72 h intravenous infusions of glucose + Intralipid in young (2-month-old) or old (6-month-old) non-diabetic Wistar rats or in 2-month-old diabetic Goto-Kakizaki rats.

The aim of this study was to compare the accuracy of multi-echo MRI, MRS and histology for the quantification of liver steatosis. We hypothesized that MR techniques would distinguish rats receiving glucose + Intralipid from those receiving saline based on their hepatic fat content. A secondary aim was to explore the link between liver steatosis assessed by MR techniques and plasma insulin/C-peptide levels.

2. Methods

2.1 Study design

All procedures were approved by the Institutional Committee for the Protection of Animals and complied with [country name withheld to maintain blinding to authors] regulatory requirements. Thirteen young Wistar (250-300 g, ∼ 8-week old, male), six old Wistar (500-600 g ∼ 26-week old, male) male rats (source omitted for submission to maintain blinding), and thirteen diabetic Goto-Kakizaki (250 g, ∼ 8-week old, male) rats (source omitted for submission to maintain blinding) were housed under controlled temperature on a 12-h light-dark cycle with unrestricted access to water and standard laboratory chow. Under general anesthesia, indwelling catheters were inserted into the left carotid artery and right jugular vein. The catheters were tunnelled subcutaneously and exteriorized at the base of the neck. The animals were allowed to recover for 5 days post surgery. Catheter patency was maintained with 50 U/ml heparin in 0.9% saline.

2.2 Rat infusions and hyperglycemic clamps

One day prior to initiating the infusion, the animals were placed in cotton vests and connected by a flexible catheter (source omitted to maintain blinding) to a single channel swivel (Harvard Apparatus, Holliston, MA) suspended above the cage. The swivel was attached to a counter-balance mounted on the top of the cage (INSTECH, Plymouth Meeting, PA), affording the animal unrestricted motion. The animals were randomized into two groups, receiving either 0.9% saline (SAL) or 70% glucose plus 20% Intralipid (GLU + IL) with 20 U/ml heparin as described by Fontés et al [22]. Plasma samples were collected from the carotid artery at the end of the 72-h infusion for insulin and C-peptide measurements [23].

2.3 Ex vivo liver preparation

At the end of the infusion, the animals were euthanized and their liver excised and immediately prepared for MRI examination. To improve field homogeneity and reduce paramagnetic susceptibility artefacts, the liver specimens were suspended in agar gel (Carolina Biological Supplies, Burlington, NC) allowing to image two livers simultaneously (Fig. 1).

2.4 MRI of liver steatosis

Hepatic fat fraction was assessed with MRI and MRS, using a 1.5 T clinical MR unit (Signa EchoSpeed 9.1; GE Medical Systems, Milwaukee, WI). A head coil was used for signal excitation and reception for MRI and MRS sequences. A transverse T1-weighted two-dimensional fast spoiled gradient-recalled dual-echo sequence was used for opposed-phase

(OP) and in-phase (IP) MRI acquisition with the following parameters: 150 ms repetition time, 2.2 and 4.5 echo times, 16 × 16 cm^2 field of view, 256 × 160 matrix, 90° flip angle, 62.5 kHz bandwidth, 2.0 mm slice thickness, 0 mm section gap, and 15 sections. An additional IP/IP T1-weighted dual-echo imaging acquisition was performed to calculate the T2* correction value using the same parameters except for 250 ms repetition time and 13.5 and 18.0 ms echo times. Data were analyzed using commercial software (ADW 4.1, GE Medical Systems, Milwaukee, WI).

Regions of interest (1.0 ± 0.1 cm^2, rectangular) were drawn in a homogeneous region of the liver on the images acquired with the IP/IP and IP/OP sequences. T2* values were calculated using the equation: $T2^* = \Delta TE / \ln(SI1/SI2)$ where ΔTE is the echo time difference between the two IP states (4.5 ms) and SI1/SI2 the ratio of the signal intensities in the two IP images. The fat fraction determined by MRI was then calculated with the equation $FF = (SI_{IP'} - SI_{OP'})/2SI_{IP'}$ where $SI_{IP'}$ and $SI_{OP'}$ are T2*-corrected signal intensities for the IP and OP images, respectively [20].

2.5 Magnetic resonance spectroscopy method

Axial T2-weighted single-shot fast spin-echo images were acquired for localization purposes before MRS data acquisition. Liver proton MRS data were acquired in a single voxel selected by a supervising radiologist. Experiments were performed using the GE PROBE SV (proton brain exam – single voxel) protocol with the voxel-selective point-resolved spectroscopy sequence and the following parameters: 1 × 1 × 1 cm^3 voxel size, 1,200 ms repetition time, 30 ms echo time, 2,500 Hz spectral width, 16 acquisitions, water suppression turned off and 22 s total acquisition time. Experiments were repeated three times in each voxel.

MR spectra were processed between 0.2 and 8.0 ppm and quantified using the LCModel software (version 6.2; S. Provencher, PhD, Oakville, Ontario, Canada) optimized for the detection of lipids in the liver (SPTYPE = 'liver-1') [24]. The simulation method quantifies the lipid signals at 0.9 (CH_3), 1.3 (CH_2) and 2.0 (CH_2) ppm after removal of the macromolecule signals. The fat fraction determined by MRS was calculated as the L/(L + W) ratio where L is the sum of the areas of the three lipid peaks and W the area of the water peak, both being corrected for T1 and T2* [20].

2.6 Histopathological analysis

Immediately after MRI and MRS examinations, excised livers were fixed in 10% buffered formalin for 24 hours at room temperature then paraffin embedded following standard procedures. Four-μm thick sections were stained with hematoxylin and eosin. The histopathological fat fraction was determined visually on the basis of the percentage of hepatocytes that contained eccentric fat vacuoles in their cytoplasm (macrosteatosis) in increments of 10%.

The radiologist and pathologist were both blinded to the results of the other examination and to the group to which the rats were allocated.

2.7 Statistical Analysis

Histopathological, MRI and MRS measurements of hepatic fat fraction, plasma insulin and C-peptide levels were expressed as their mean and median with standard deviation in parentheses. Since the fat fraction was not normally distributed, analysis was performed using non-parametric tests. Wilcoxon rank sum tests were used to test for differences in the fat fraction (as measured by MRI, MRS, and histopathology) between the infusion groups (SAL versus GLU + IL), overall, and for each of the three phenotypes (young Wistar, old

Wistar, Goto-Kakizaki). Regression analysis and Pearson correlation coefficients were used to assess the correlation between different fat quantification techniques as well as between MR fat quantification techniques, plasma insulin and C-peptide levels. The agreement between MRI, MRS, and histopathology for the assessment of liver fat fraction were reported as bias ± 1.96 standard deviations of the differences, followed by the 95% limits of agreement interval according to the Bland-Altman method. Within-subject analysis was performed by using Friedman tests to compare the fat quantification techniques. Post-hoc analysis with Wilcoxon signed-rank tests was conducted with a Bonferroni correction applied. Accuracy, sensitivity, and specificity of fat quantification techniques were calculated for detection of 5% fat fraction with area under the receiver operating characteristic (ROC) curve. p values < 0.05 were considered significant. Statistical analyses were performed with R Development Core Team (2011) software (R Foundation for Statistical Computing, Vienna, Austria) and SPSS, version 20.0; SPSS, Chicago, Ill).

3. Results

3.1 Steatosis induction with glucolipotoxic model

MRI, MRS and histopathology results in the SAL and GLU + IL groups are summarized in Table 1. MRI, MRS and histopathology accurately distinguished the rats (all groups pooled) receiving the infusion of GLU + IL from those receiving the SAL control with p values < 0.01.

3.2 Steatosis response of different phenotypes

Differences in FF values between the three different rat phenotypes submitted to two infusion protocols (SAL or GLU + IL) for the different fat quantification methods are shown in Figure 2. MRI and MRS were able to discriminate between the GLU+IL and SAL groups for the Goto-Kakizaki and young Wistar populations whereas no significant difference was found for the old Wistar rat group. Although histopathological evaluation showed a trend toward increased FF in GLU + IL groups, no statistically significant differences were detected.

3.3 Correlation between MRI, MRS and histopahological results

A strong correlation was found between MRI-FF and MRS-FF (r = 0.81, p < 0.01). A weaker correlation was found between histopathological FF and MRS-FF (r = 0.60, p < 0.01). The slope and intercept values were 0.76 and -1.1 (p < 0.01), respectively, for MRI-FF data, 0.36 and 2.8 (p < 0.01), respectively, for the histopathological FF data.

3.4 Agreement between MRI, MRS and histopahological results

Bland-Altman analysis showed trends toward agreement between histopathological assessment and MRS-FF (mean bias 0.13%). The limits of agreement (±1.96) between the two fat quantification methods were wide: -10.37% to 10.62%. Bland-Altman analysis also showed trends toward agreement between histopathological assessment and MRI-FF (mean bias -2.77%). The limits of agreement (±1.96) between the two fat quantification methods were wide: -13.02% to 7.49%. Further, Bland-Altman analysis indicated good agreement, with a small positive bias between MRI-FF and MRS-FF (mean bias 2.89%). The limits of agreement were narrower than for histopathology: -2.19% to 7.97% (Fig. 3).

3.5 Within-subject analysis

Within-subject analysis showed significant differences in fat fraction depending on the fat quantification technique used, $\chi^2(2) = 18.47$, p < 0.001. Median (IQR) fat fraction for MRI, MRS, and histopathology were 6.33% (3.54% to 10.43%), 5.00% (0.81% to 7.70%), and

2.00% (0.00% to 10.00%), respectively. There were no significant differences in fat quantification between histopathology and MRS-FF (Z = -0.335, p = 0.738). However, there were statistically significant differences in fat quantification between MRI-FF and MRS-FF (Z = -4.357, p < 0.001) and between histopathology and MRI-FF (Z = -2.842, p = 0.004).

3.6 Diagnostic accuracy of fat quantification techniques

Estimates of accuracy, sensitivity, and specificity to detect significant steatosis were calculated using ROC analysis. To distinguish a 5% FF threshold for significant steatosis using MRS as the reference standard, the area under the ROC curves was 0.841 (95% confidence interval [CI]: 0.705 to 0.978) for MRI and 0.641 (95% CI: 0.441 to 0.841) for histopathology. The sensitivity was 92.9% (95% CI: 68.5% to 98.7%) for MRI and 50.0% (95% CI: 26.8% to 73.3%) for histopathology. The specificity was 55.6% (95% CI: 33.7% to 75.4%) for MRI and 72.2% (95% CI: 49.1% to 87.5%) for histopathology.

3.8 Correlation between liver fat fraction, insulin and C-peptide levels

The mean and median (SD) insulin secretion levels at the end of the infusion were 1825.1 and 1394.6 (1584.0) pmol/l, respectively, for the GLU+IL group and 309.9 and 378.8 (189.4) pmol/l, respectively, for the SAL group. The mean and median C-peptide concentrations were 2.874 and 2.882 (0.916) nmol/l, respectively, for the GLU+IL group and 2.276 and 1.668 (1.291) nmol/l, respectively for the SAL group. Pearson correlation coefficients were 0.63 (p < 0.01) between MRI-FF and insulin level, 0.57 (p < 0.01) between MRS-FF and insulin level was, and 0.36 (p = 0.06) between histology-FF and insulin level. Pearson correlation coefficients were 0.54 (p < 0.01) between MRI-FF and C-peptide concentration, 0.44 (p = 0.02) between MRS-FF and C-peptide concentration, and 0.11 (p = 0.58) between histology-FF and C-peptide.

4. Discussion

In this study, the ability of two noninvasive MR methods (MRI and MRS) to measure early onset of liver steatosis in a rodent glucolipotoxic diabetic model and their correlation with insulin/C-peptide plasma level has been demonstrated. To our knowledge, this is the first study to evaluate the ability of MR-based liver fat quantification methods in an experimetal glucolipotoxic diabetic model. This is important because early detection of liver steatosis has clinical implications for risk prediction of type 2 diabetes, prior to development of major co-morbidities associated with type 2 diabetes or NAFLD.

Our work demonstrated that MRS and MRI accurately distinguished rats receiving GLU + IL infusions from those receiving SAL control. Among the three rat phenotypes, only the old Wistar rats did not reveal significant fat fraction differences between the SAL- and GLU +IL-infused rats, most likely due to preexisting steatosis in old Wistar rats (mean 3.9 % compared to 0.8 % in young Wistar and 0.0 % in Goto-Kakizaki as assessed by MRS). Also, there were only 6 old Wistar rats and therefore only 3 per group. Thus, the small number of old Wistar rats limits our ability to make meaningful inferences about our ability to detect differences in liver fat fraction between the rats randomized to the SAL- or GLU+IL groups.

In contrast to MR techniques, histopathology failed to demonstrate significant fat differences between the two infusion regimens for each individual rat phenotype. One potential explanation for the poorer results obtained with histopathology compared to MR-based techniques is that visual semi-quantitative histologic analysis of percentage of fatty hepatocytes, even in 10% increments, cannot discriminate subtle differences in steatosis, unlike continuous values of fat content obtained with MR techniques [21]. Furthermore, the invasive nature of liver biopsy makes it unsuitable for detection of early liver steatosis.

Our results in a glucolipotoxic model of subtle steatosis confirm the usefulness of MR techniques for liver fat quantification, as reported previously in other animal models of steatosis [25, 26]. MRI-FF has been shown to strongly correlate with lipid concentration performed on liver extracts in overfed Wistar rats and in an ob/ob mouse model of hepatic steatosis [25, 26]. The feasibility of MRI-based liver fat quantification was previously demonstrated in a cross-sectional study comparing control and steatotic Wistar rats [25]. MRI-based liver fat quantification was proposed as a noninvasive alternative to biopsy in a wide range of steatosis *in vivo* [26]. Furthermore, noninvasive assessment of fat fraction in animal models allows longitudinal evaluation. For instance, Marsman et al. used MRS in Wistar rats to quantify steatosis induced by a methionine/choline-deficient diet and steatosis reversal obtained by omega-3 fatty acid administration [27].

A strong correlation was found between MRI-FF and MRS-FF in our study. Proton magnetic resonance spectroscopy (MRS) is widely considered as the most accurate noninvasive technique for hepatic fat quantification [28, 29]. Using MRS as our reference, the feasibility and accuracy of a multi-echo MRI technique for the quantification of *ex vivo* rat liver fat fraction could be demonstrated in a clinical MR imager.

We evaluated the inter-technique agreement for hepatic fat quantification. Trends toward agreement were found between histological assessment and MRS-FF, and between histological assessment and MRI-FF. Also, a small bias was found between MRI-FF and MRS-FF. However, the inter-technique limits of agreement were wider for the comparison between histopathology and MRS, and between histopathology and MRI than for MRI and MRS. This difference is anticipated since histopathology evaluates fat content as the amount of fat per surface unit area, whereas both MRI and MRS evaluate fat content as the amount of fat per volume unit area. Hence, closer limits of agreement are expected for the two MR-based fat quantification techniques.

In our study, the goal was not to directly induce steatosis, but to induce insulin resistance and glucolipotoxicity using a validated model of GLU + IL infusions [22] and analyze early steatosis. The originality of our work is based on the demonstration that a widely available MRI method can measure small to moderate amounts of liver fat (mean 6.6 % with MRS) more accurately than histopathology in diabetic rats.

Our study also showed a close correlation between hepatic FF as measured by MR techniques and insulin/C-peptide plasma levels. This is consistent with the known correlation between insulin resistance and liver steatosis [3, 12, 30-32]. This complex link between glucose homeostasis and liver steatosis has been shown by various approaches. First, steatosis appears early in the natural history of type 2 diabetes during the preclinical phase and may regress in parallel to diabetes resolution, for instance after bariatric surgery [33]. Several potential mechanisms have been proposed, suggesting that insulin resistance may be the pathogenic condition responsible for both metabolic diseases and NAFLD [32-34]. Second, increased liver fat assessed by MRS has been shown to be associated with impaired insulin clearance and hepatic and adipose tissue insulin resistance in type 2 diabetes patients [3, 30]. Interestingly, the link between insulin-resistance and fat accumulation in the liver seems to be independent of body mass index and intra-abdominal obesity in adults and adolescents [31, 35, 36]. Third, the role of insulin resistance in NAFLD is also supported by therapeutic studies [37-39]. In an animal model of NAFLD in obese, leptin-deficient mice, metformin, an insulin-sensitizing agent, significantly reduced steatosis, hepatomegaly and aminotransferase levels [37]. A recent randomized, placebo-controlled trial confirmed the ability of metformin to improve liver function in patients with NAFLD [40]. In patients with type 2 diabetes, moderate weight loss reversed hepatic insulin resistance, normalized fasting hyperglycemia and reduced hepatic fat content by 81 ± 4 %

[38]. Most of these studies were based on MRS or histology for fat quantification but none used widely available multi-echo MRI.

Our study entailed some limitations. First, MRI quantification was performed on *ex vivo* livers, which introduces potential caveats associated with tissue conservation and non-physiological temperature [26]. We anticipate equivalent or superior results with *in vivo* MRI. Second, correction of the MRI signals for T1 differences between water and fat was not performed. The use of lower flip angles has been recommended to decrease the T1-weighting of the multi-echo MR sequence [19]. However, the limited signal-to-noise ratio obtained in this rat study performed at 1.5T did not allow us to use a lower flip angle. This may explain why our MRI-MRS correlations were lower than those previously published [19, 25, 26, 41]. Despite these limitations, a good discrimination was obtained between SAL- and GLU + IL-infused rats. Third, lipid extractions were not carried out on liver specimens for biochemical quantification. However, a previous study has demonstrated excellent correlations between MRS-FF and fat percentage measured by gas chromatography on liver extracts which supports the validity of MRS [41, 42].

In conclusion, our results suggest that multi-echo MRI and MRS are accurate methods for the detection of early steatosis in an experimental glucolipotoxic rat model. The good correlation between insulin levels and MRI-FF advocates the use of the widely available and noninvasive MRI technique to explore the relationship between glucose metabolism and hepatic fat content.

Acknowledgments

We thank R. Rabasa-Lhoret, MD, PhD, for his advice with the manuscript preparation.

Grant support: Funding: Funding for this project was supported by: (1) the U.S. National Institutes of Health (R01DK58096 to V. Poitout); (2) the Canadian Institutes of Health Research (MOP 77686 to V. Poitout); (3) the Canadian Diabetes Association (post-doctoral fellowship to G. Fontés); (4) the Société Française de Radiologie (clinical research scholarship to G. d'Assignies) and (5) a clinical research award from Fonds de la recherche du Québec en santé (FRQ-S to An Tang).

References

1. Shibata M, Kihara Y, Taguchi M, et al. Nonalcoholic fatty liver disease is a risk factor for type 2 diabetes in middle-aged japanese men. Diabetes Care. 2007; 30(11):2940–4. [PubMed: 17666460]
2. Bae JC, Rhee EJ, Lee WY, et al. Combined effect of nonalcoholic fatty liver disease and impaired fasting glucose on the development of type 2 diabetes: A 4-year retrospective longitudinal study. Diabetes Care. 2011; 34(3):727–9. [PubMed: 21278140]
3. Kotronen A, Juurinen L, Hakkarainen A, et al. Liver fat is increased in type 2 diabetic patients and underestimated by serum alanine aminotransferase compared with equally obese nondiabetic subjects. Diabetes Care. 2008; 31(1):165–9. [PubMed: 17934148]
4. Younossi ZM, Otgonsuren M, Venkatesan C, et al. In patients with non-alcoholic fatty liver disease, metabolically abnormal individuals are at a higher risk for mortality while metabolically normal individuals are not. Metabolism. 2013; 62(3):352–60. [PubMed: 22999011]
5. Adams LA, Talwalkar JA. Diagnostic evaluation of nonalcoholic fatty liver disease. J Clin Gastroenterol. 2006; 40(3 Suppl 1):S34–8. [PubMed: 16540765]
6. Angulo P. Nonalcoholic fatty liver disease. N Engl J Med. 2002; 346(16):1221–31. [PubMed: 11961152]
7. Cusi K. Nonalcoholic fatty liver disease in type 2 diabetes mellitus. Curr Opin Endocrinol Diabetes Obes. 2009; 16(2):141–9. [PubMed: 19262374]
8. Leite NC, Villela-Nogueira CA, Pannain VL, et al. Histopathological stages of nonalcoholic fatty liver disease in type 2 diabetes: Prevalences and correlated factors. Liver Int. 2011; 31(5):700–6. [PubMed: 21457442]

9. Preiss D, Sattar N. Non-alcoholic fatty liver disease: An overview of prevalence, diagnosis, pathogenesis and treatment considerations. Clin Sci (Lond). 2008; 115(5):141–50. [PubMed: 18662168]
10. El-Serag HB, Tran T, Everhart JE. Diabetes increases the risk of chronic liver disease and hepatocellular carcinoma. Gastroenterology. 2004; 126(2):460–8. [PubMed: 14762783]
11. Gariani K, Philippe J, Jornayvaz FR. Non-alcoholic fatty liver disease and insulin resistance: From bench to bedside. Diabetes Metab. 2012
12. Jacobs M, van Greevenbroek MM, van der Kallen CJ, et al. The association between the metabolic syndrome and alanine amino transferase is mediated by insulin resistance via related metabolic intermediates (the cohort on diabetes and atherosclerosis maastricht [codam] study). Metabolism. 2011; 60(7):969–75. [PubMed: 21040936]
13. El-Badry AM, Breitenstein S, Jochum W, et al. Assessment of hepatic steatosis by expert pathologists: The end of a gold standard. Ann Surg. 2009; 250(5):691–7. [PubMed: 19806055]
14. Ratziu V, Charlotte F, Heurtier A, et al. Sampling variability of liver biopsy in nonalcoholic fatty liver disease. Gastroenterology. 2005; 128(7):1898–906. [PubMed: 15940625]
15. Regev A, Berho M, Jeffers LJ, et al. Sampling error and intraobserver variation in liver biopsy in patients with chronic hcv infection. Am J Gastroenterol. 2002; 97(10):2614–8. [PubMed: 12385448]
16. Belfort R, Harrison SA, Brown K, et al. A placebo-controlled trial of pioglitazone in subjects with nonalcoholic steatohepatitis. N Engl J Med. 2006; 355(22):2297–307. [PubMed: 17135584]
17. Szczepaniak LS, Nurenberg P, Leonard D, et al. Magnetic resonance spectroscopy to measure hepatic triglyceride content: Prevalence of hepatic steatosis in the general population. Am J Physiol Endocrinol Metab. 2005; 288(2):E462–8. [PubMed: 15339742]
18. Reeder SB, Robson PM, Yu H, et al. Quantification of hepatic steatosis with mri: The effects of accurate fat spectral modeling. J Magn Reson Imaging. 2009; 29(6):1332–9. [PubMed: 19472390]
19. Yokoo T, Bydder M, Hamilton G, et al. Nonalcoholic fatty liver disease: Diagnostic and fat-grading accuracy of low-flip-angle multiecho gradient-recalled-echo mr imaging at 1.5 t. Radiology. 2009; 251(1):67–76. [PubMed: 19221054]
20. d'Assignies G, Ruel M, Khiat A, et al. Noninvasive quantitation of human liver steatosis using magnetic resonance and bioassay methods. Eur Radiol. 2009; 19(8):2033–40. [PubMed: 19280194]
21. Guiu B, Petit JM, Loffroy R, et al. Quantification of liver fat content: Comparison of triple-echo chemical shift gradient-echo imaging and in vivo proton mr spectroscopy. Radiology. 2009; 250(1):95–102. [PubMed: 19092092]
22. Fontes G, Zarrouki B, Hagman DK, et al. Glucolipotoxicity age-dependently impairs beta cell function in rats despite a marked increase in beta cell mass. Diabetologia. 2010; 53(11):2369–79. [PubMed: 20628728]
23. Hagman DK, Latour MG, Chakrabarti SK, et al. Cyclical and alternating infusions of glucose and intralipid in rats inhibit insulin gene expression and pdx-1 binding in islets. Diabetes. 2008; 57(2): 424–31. [PubMed: 17991758]
24. Provencher SW. Estimation of metabolite concentrations from localized in vivo proton nmr spectra. Magn Reson Med. 1993; 30(6):672–9. [PubMed: 8139448]
25. Hijona E, Sanchez-Gonzalez J, Alustiza JM, et al. Accurate fat fraction quantification by multiecho gradient-recalled-echo magnetic resonance at 1.5t in rats with nonalcoholic fatty liver disease. Eur J Radiol. 2011; 81(6):1122–7. [PubMed: 21459536]
26. Hines CD, Yu H, Shimakawa A, et al. Quantification of hepatic steatosis with 3-t mr imaging: Validation in ob/ob mice. Radiology. 2010; 254(1):119–28. [PubMed: 20032146]
27. Marsman HA, Heger M, Kloek JJ, et al. Reversal of hepatic steatosis by omega-3 fatty acids measured non-invasively by (1) h-magnetic resonance spectroscopy in a rat model. J Gastroenterol Hepatol. 2010; 26(2):356–63. [PubMed: 21261727]
28. Fischbach F, Bruhn H. Assessment of in vivo 1h magnetic resonance spectroscopy in the liver: A review. Liver Int. 2008; 28(3):297–307. [PubMed: 18290772]
29. Joy D, Thava VR, Scott BB. Diagnosis of fatty liver disease: Is biopsy necessary? Eur J Gastroenterol Hepatol. 2003; 15(5):539–43. [PubMed: 12702913]

30. Kotronen A, Juurinen L, Tiikkainen M, et al. Increased liver fat, impaired insulin clearance, and hepatic and adipose tissue insulin resistance in type 2 diabetes. Gastroenterology. 2008; 135(1): 122–30. [PubMed: 18474251]
31. Seppala-Lindroos A, Vehkavaara S, Hakkinen AM, et al. Fat accumulation in the liver is associated with defects in insulin suppression of glucose production and serum free fatty acids independent of obesity in normal men. J Clin Endocrinol Metab. 2002; 87(7):3023–8. [PubMed: 12107194]
32. Ardigo D, Numeroso F, Valtuena S, et al. Hyperinsulinemia predicts hepatic fat content in healthy individuals with normal transaminase concentrations. Metabolism. 2005; 54(12):1566–70. [PubMed: 16311087]
33. Taylor R. Pathogenesis of type 2 diabetes: Tracing the reverse route from cure to cause. Diabetologia. 2008; 51(10):1781–9. [PubMed: 18726585]
34. Bugianesi E, Zannoni C, Vanni E, et al. Non-alcoholic fatty liver and insulin resistance: A cause-effect relationship? Digestive and Liver Disease. 2004; 36(3):165–73. [PubMed: 15046183]
35. Chitturi S, Abeygunasekera S, Farrell GC, et al. Nash and insulin resistance: Insulin hypersecretion and specific association with the insulin resistance syndrome. Hepatology. 2002; 35(2):373–9. [PubMed: 11826411]
36. Perseghin G, Bonfanti R, Magni S, et al. Insulin resistance and whole body energy homeostasis in obese adolescents with fatty liver disease. Am J Physiol Endocrinol Metab. 2006; 291(4):E697–703. [PubMed: 16684857]
37. Lin HZ, Yang SQ, Chuckaree C, et al. Metformin reverses fatty liver disease in obese, leptin-deficient mice. Nat Med. 2000; 6(9):998–1003. [PubMed: 10973319]
38. Petersen KF, Dufour S, Befroy D, et al. Reversal of nonalcoholic hepatic steatosis, hepatic insulin resistance, and hyperglycemia by moderate weight reduction in patients with type 2 diabetes. Diabetes. 2005; 54(3):603–8. [PubMed: 15734833]
39. Tsuchida T, Shiraishi M, Ohta T, et al. Ursodeoxycholic acid improves insulin sensitivity and hepatic steatosis by inducing the excretion of hepatic lipids in high-fat diet-fed kk-ay mice. Metabolism. 2012; 61(7):944–53. [PubMed: 22154323]
40. Sofer E, Boaz M, Matas Z, et al. Treatment with insulin sensitizer metformin improves arterial properties, metabolic parameters, and liver function in patients with nonalcoholic fatty liver disease: A randomized, placebo-controlled trial. Metabolism. 2011; 60(9):1278–84. [PubMed: 21411114]
41. Marsman HA, van Werven JR, Nederveen AJ, et al. Noninvasive quantification of hepatic steatosis in rats using 3.0 t 1h-magnetic resonance spectroscopy. J Magn Reson Imaging. 2010; 32(1):148–54. [PubMed: 20578022]
42. van Werven JR, Marsman HA, Nederveen AJ, et al. Hepatic lipid composition analysis using 3.0-t mr spectroscopy in a steatotic rat model. Magn Reson Imaging. 2012; 30(1):112–21. [PubMed: 21940131]

Abbreviations

FF	Fat fraction
GLU+IL	Glucose + Intralipid
IP	In-phase
MR	Magnetic resonance
MRI	Magnetic resonance imaging
MRS	Magnetic resonance spectroscoy
NAFLD	Nonalcoholic fatty liver disease
NASH	Nonalcoholic steatohepatitis
OP	Opposed-phase

ROC	Receiver operating characteristic
SAL	Saline

1a.

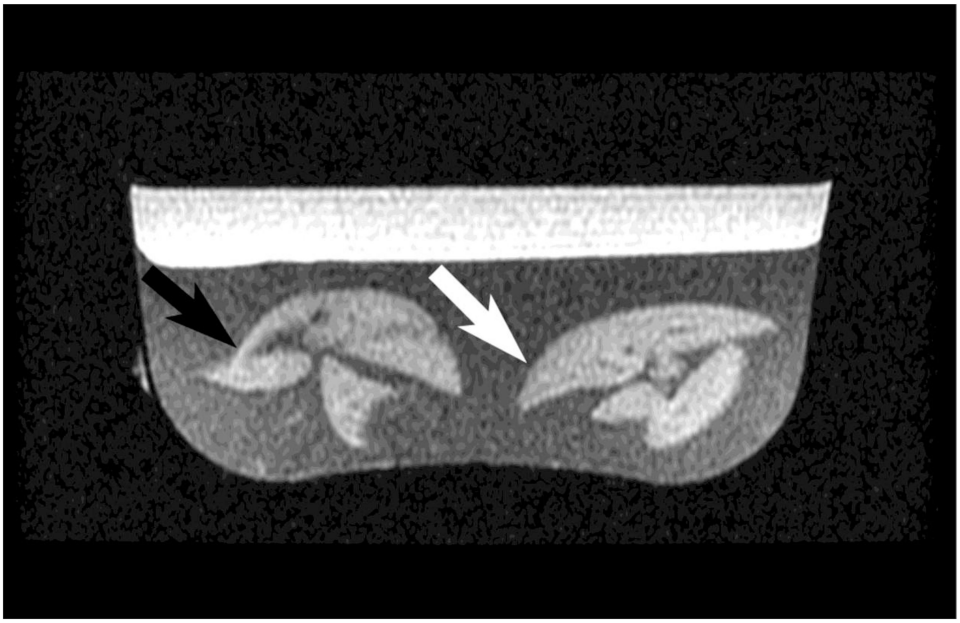

1b.

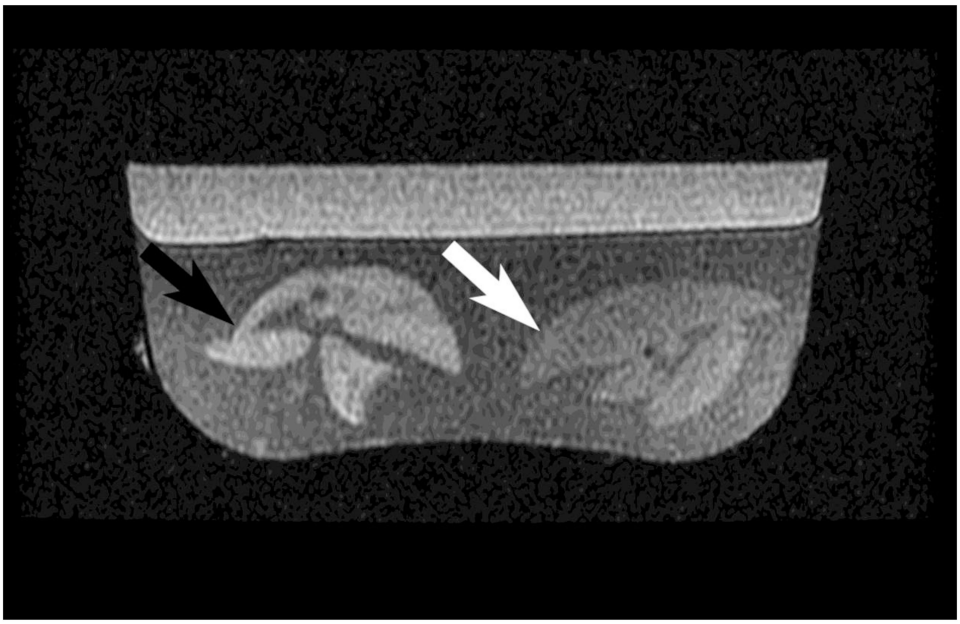

Fig. 1.

Two rat liver specimens prepared in agar and imaged with gradient-echo in-phase (4.5 ms echo time) (**A**) and out-of-phase (2.2 ms echo time) (**B**) sequences in a clinical 1.5 T MR scanner. The rat liver on the left was collected following saline (SAL; black arrow) infusion and the other following glucose and Intralipid (GLU + IL; white arrow) fat emulsion infusion. T2* corrected fat fractions were 4.8 % for SAL and 15.9 % for GLU + IL.

2a.

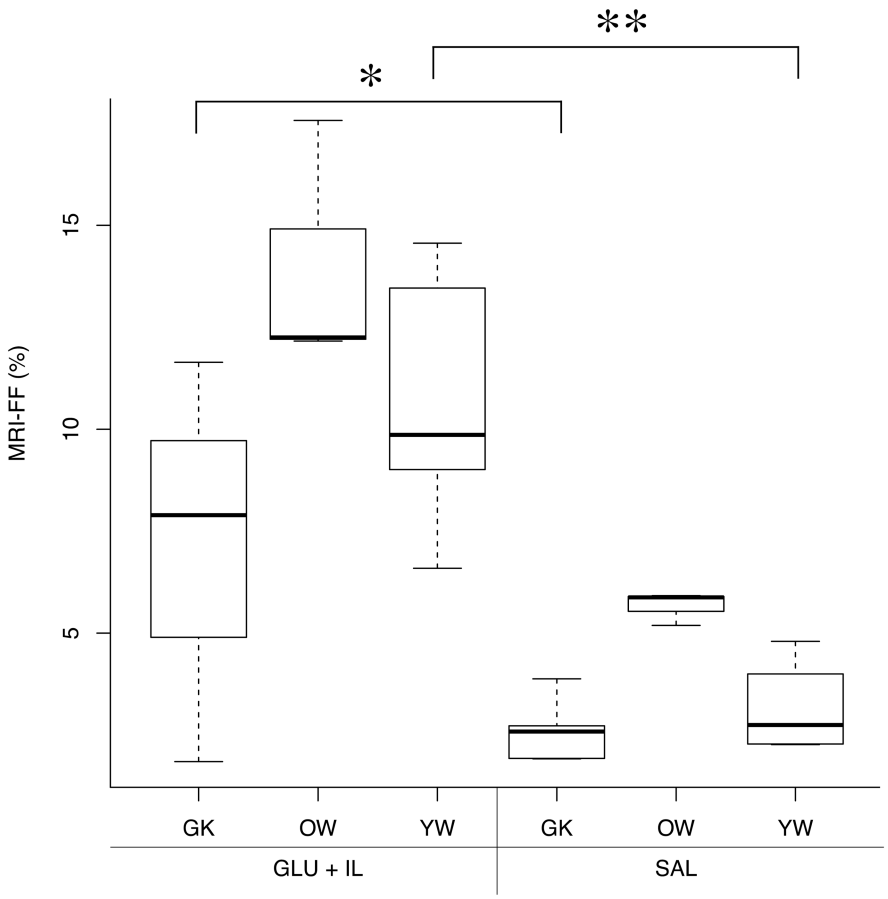

2b.

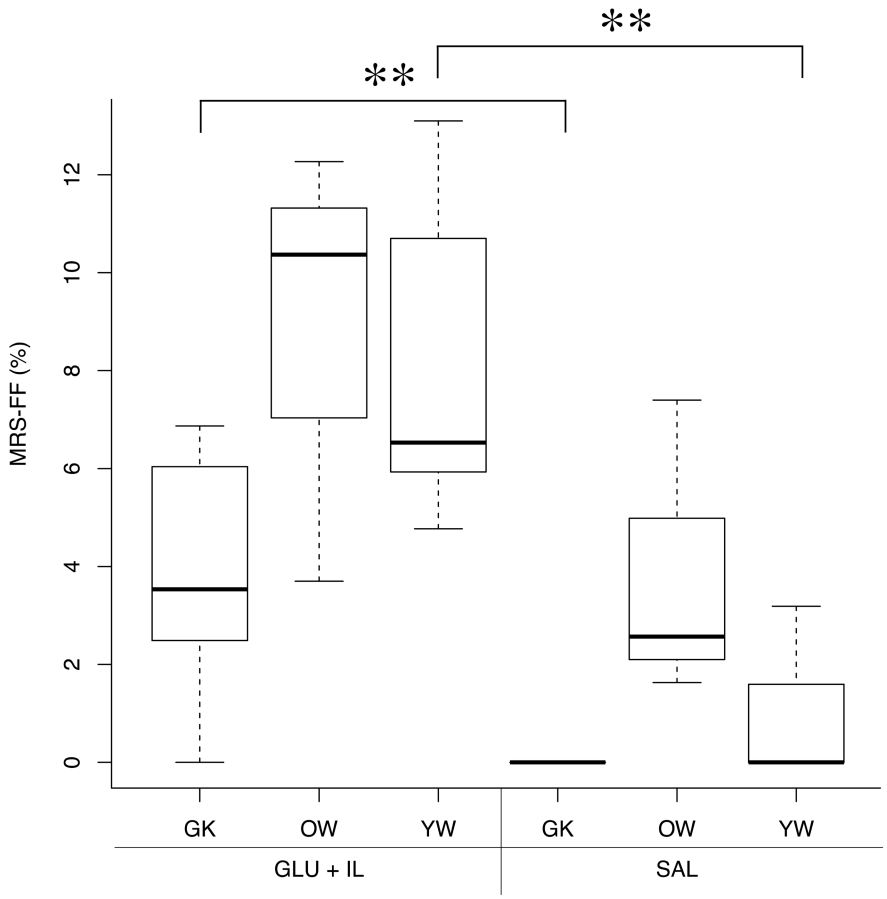

2c.

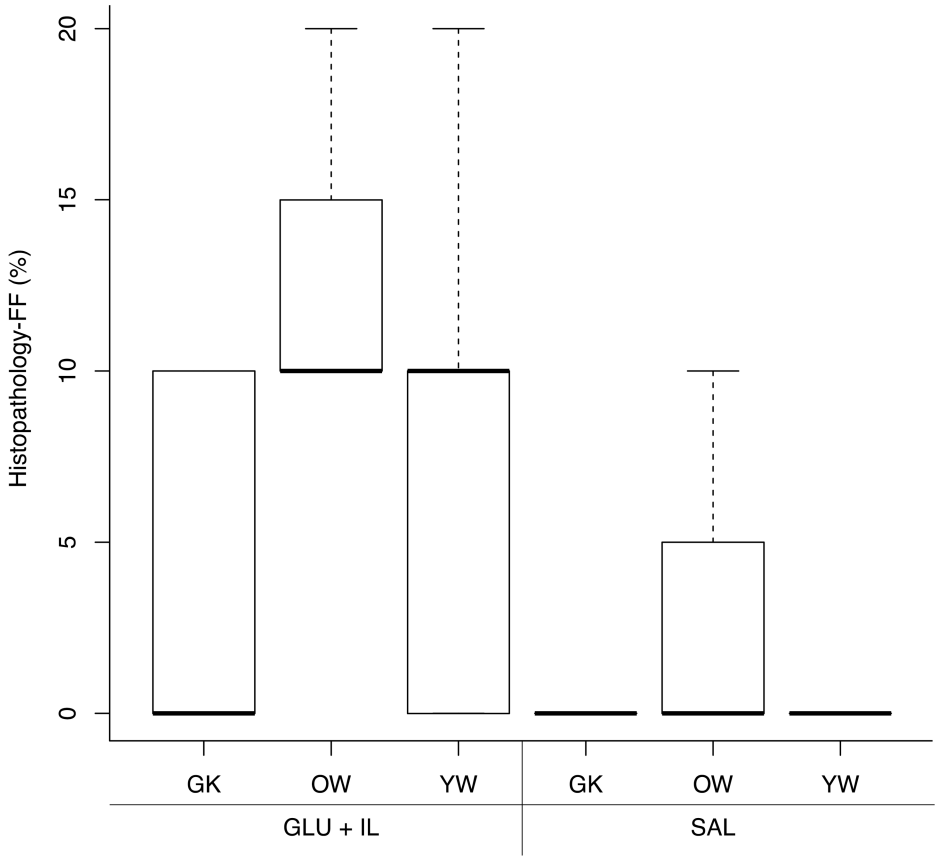

Fig. 2.

Boxplots of liver fat fraction (%) as determined by magnetic resonance imaging (MRI) (**A**), magnetic resonance spectroscopy (MRS) (**B**) and histopathology (**C**) for the three rat phenotypes: young Wistar (YW), old Wistar (OW) and Goto-Kakizaki (GK) infused with two types of solution: saline control (SAL) and glucose + Intralipid fat emulsion (GLU+IL). Boxplots show median (horizontal lines in boxes) and quartiles. Whiskers extend to the most extreme observations that are not more than 1.5 × interquartile range beyond the quartiles. *$p < 0.05$, ** $p < 0.01$.

3a.

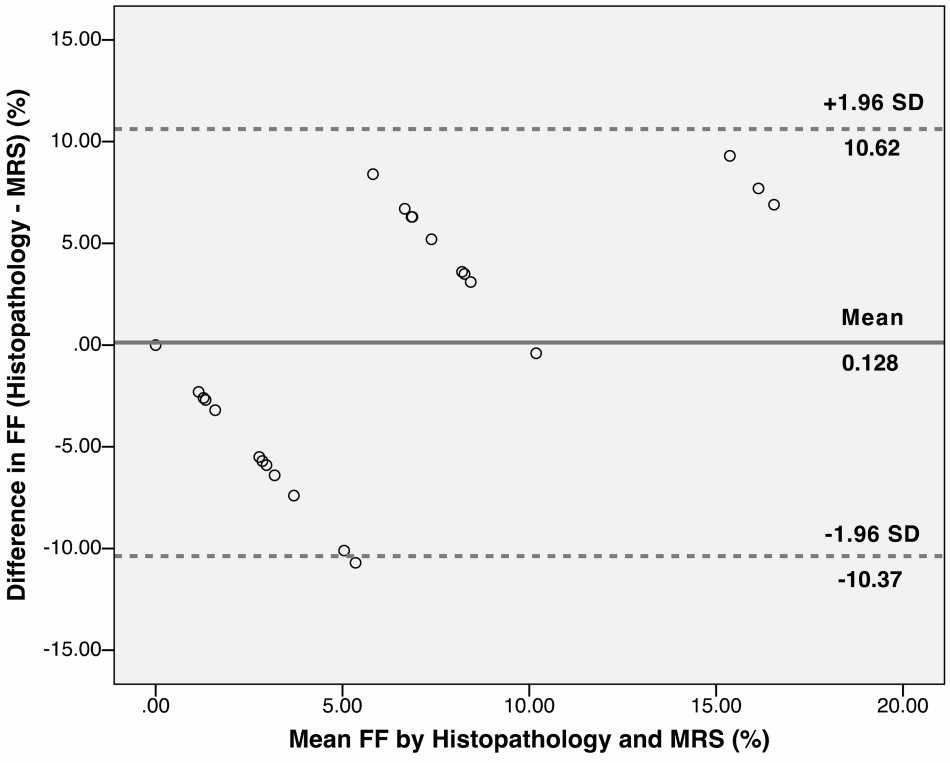

3b.

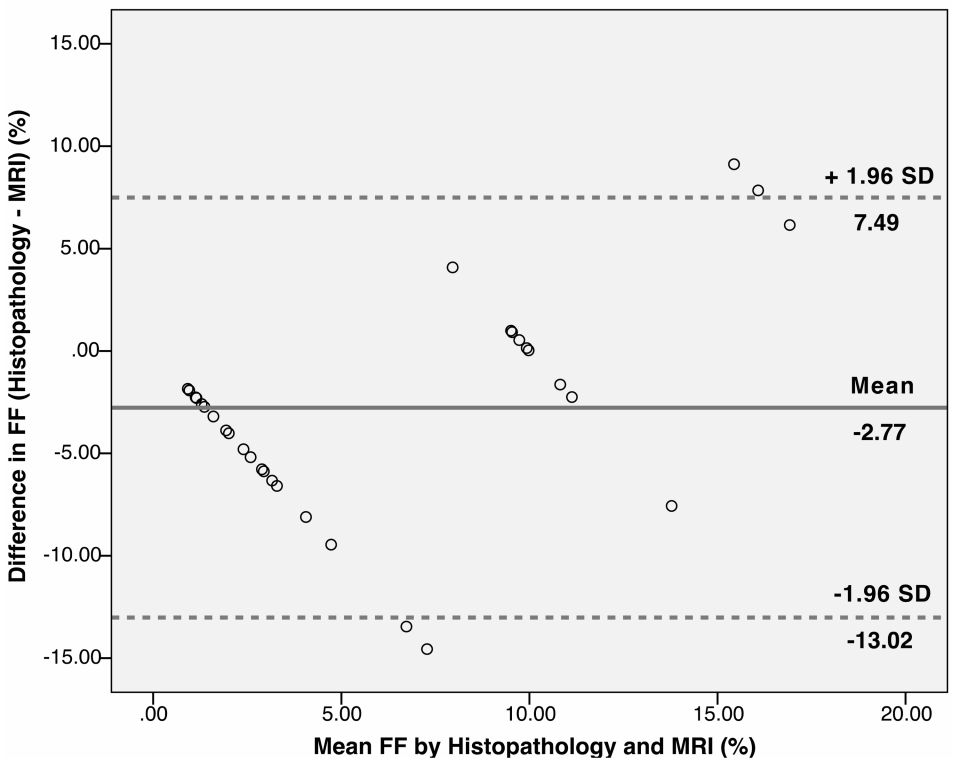

3c.

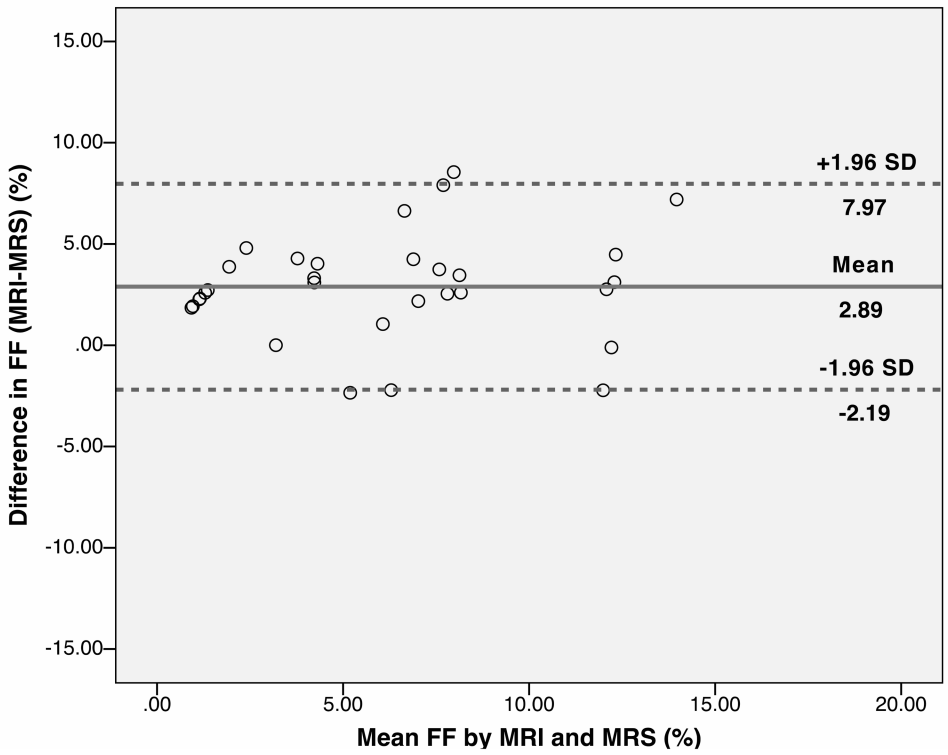

Fig. 3.

Bland-Altman plots show the difference between the percentage of hepatocytes with macrovesicular steatosis as determined by histopathology and magnetic resonance spectroscopy (MRS)-determined fat fraction plotted against their mean (**A**), between histopathology and magnetic resonance imaging (MRI) fat fractions (**B**), and between the MRI and the MRS fat fractions (**C**) in rat livers. The central lines indicate bias, and outer lines indicate limits of agreement (±1.96 standard deviations).

Table 1

Comparison of MRI, MRS and histopathological fat fraction between saline and glucose + Intralipid infusions groups

	SAL (n=12)	GLU+IL (n=20)	*p*
MRI-FF (%)	3.5 (3.0) [1.5]	9.8 (9.7) [3.8]	< 0.01
MRS-FF (%)	1.2 (0.0) [2.3]	6.6 (6.1) [3.6]	< 0.01
HIS-FF (%)	0.8 (0.0) [2.9]	7.0 (10.0) [7.3]	< 0.01

Data are means, with medians in parentheses and standard deviation in brackets. SAL = saline. GLU + IL = glucose + Intralipid. MRI-FF = magnetic resonance imaging fat fraction. MRS-FF = magnetic resonance spectroscopy fat fraction. HIS-FF = histopathology fat fraction.